ACS Infectious Diseases

pubs.acs.org/journal/aidcbc

Letter

Target-Based Design of Promysalin Analogues Identifies a New Putative Binding Cleft in Succinate Dehydrogenase

Savannah J. Post,[⊥] Colleen E. Keohane,[⊥] Lauren M. Rossiter, Anna R. Kaplan, Jittasak Khowsathit, Katie Matuska, John Karanicolas, and William M. Wuest*

Cite This: https://dx.doi.org/10.1021/acsinfecdis.0c00024

Read Online

ACCESS | Metrics & More | Article Recommendations | Supporting Information

ABSTRACT: Promysalin is a small-molecule natural product that specifically inhibits growth of the Gram-negative pathogen *Pseudomonas aeruginosa* (*PA*). This activity holds promise in the treatment of multidrug resistant infections found in immunocompromised patients with chronic illnesses, such as cystic fibrosis. In 2015, our lab completed the first total synthesis; subsequent analogue design and SAR investigation enabled identification of succinate dehydrogenase (Sdh) as the biological target in *PA*. Herein, we report the target-guided design of new promysalin analogues with varying alkyl chains, one of which is on par with our most potent analogue to date. Computational docking revealed that some analogues have a different orientation in the Sdh binding pocket, placing the terminal carbon proximal to a tryptophan residue. This inspired the design of an extended side chain analogue bearing a terminal phenyl moiety, providing a basis for the design of future analogues.

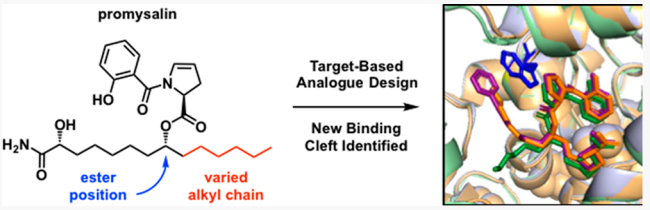

KEYWORDS: *antibiotics, Pseudomonas aeruginosa, succinate dehydrogenase, diverted total synthesis, molecular modeling*

Since the introduction of penicillin into hospitals in 1943, antibiotics have played an instrumental role in the treatment of bacterial infections.[1] Despite this success, the threat of antibiotic-resistant microbes continues to increase. According to the recent report by the CDC, there are over 2.8 million cases of antibiotic-resistant infections reported annually, resulting in more than 35 000 deaths.[2] One cause of antibiotic resistance is the misuse and overprescription of clinical antibiotics, most of which are broad-spectrum, meaning they target a wide range of bacterial species.[3] While broad spectrum therapeutics are beneficial when the identity of the infecting pathogen is unknown, their use eradicates all susceptible bacteria, increasing nutrient availability to resistant microbes and enabling them to proliferate rapidly.[4,5] This is particularly problematic for patients with compromised immune systems, as they are unable to fend off infections without heavy, prolonged use of broad-spectrum antibiotics.

Particularly at risk by this extensive use of broad-spectrum antibiotics are patients with cystic fibrosis (CF), which is caused by a defect in the gene encoding the CFTR (cystic fibrosis transmembrane conductance regulator) protein. This disease results in the buildup of thick mucus layers in the lungs,[6] providing harmful pathogens such as *Staphylococcus aureus* and *Pseudomonas aeruginosa* (*PA*) with an ideal environment for colonization and infection. Once colonized, patients are required to continuously take high doses of antibiotics for the entirety of their lives.[7] Accompanying this extensive antibiotic treatment is the emergence of multidrug-resistant *PA*, with an estimated 32 600 cases reported in hospitalized patients, resulting in 2 700 deaths and costing the public $767 million in 2017.[8]

These problems have triggered a renewed effort to develop narrow-spectrum antibiotics, defined as being active against only Gram-positive or only Gram-negative bacteria, to combat these resistant microbes.[9] An even more effective tactic to avoid both resistance development and collateral damage to commensal species would be the use of species-specific antibiotics, especially for colonized CF patients, for which 80% are infected by *PA* by the age of 18.[10] As a result, our group has become interested in the prospect of developing an antibiotic that is active solely against *PA*. This goal is quite daunting, due to the complex nature of bacteria, their ability to rapidly adapt, and the significant overlap in biological targets. We expected to find such specificity in nature, particularly in the rhizosphere where Gram-negative pathogens like *PA* thrive. We sought inspiration from recently characterized natural products to fill this scientific gap.[11−13]

In 2011, De Mot and co-workers isolated a new metabolite from *Pseudomonas putida*, promysalin ((−)-**1**, Figure 1A), which was shown to selectively inhibit the growth of *PA*, despite being tested against a wide variety of other Gram-

Special Issue: Antibiotics

Received: January 15, 2020

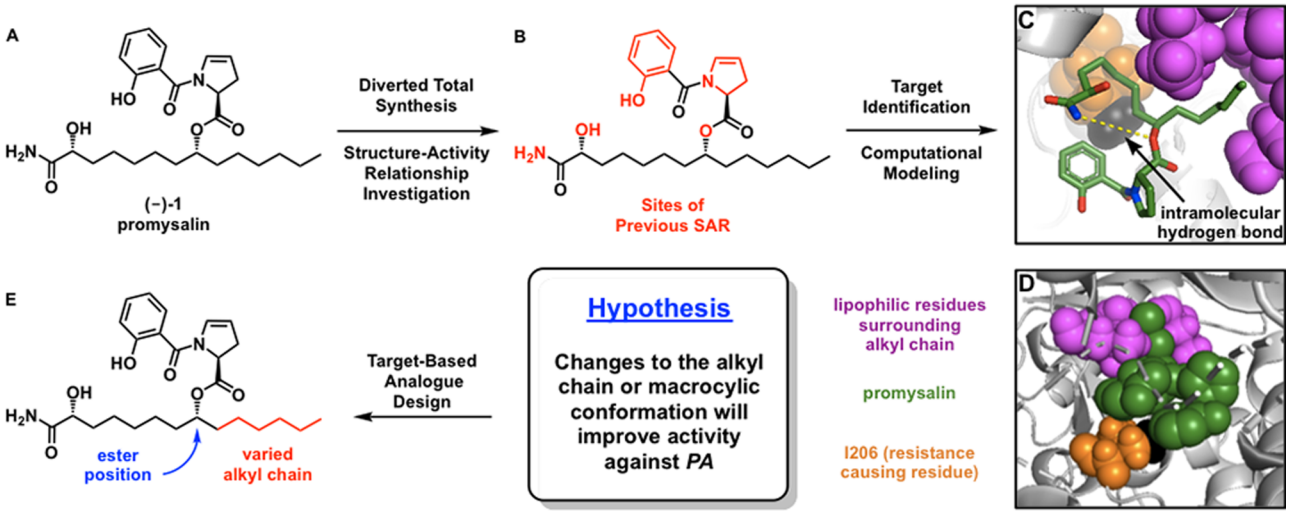

Figure 1. (A) Structure of promysalin. (B) Summary of moieties modified in previous SAR. (C) Computational docking of promysalin (green) in Sdh highlighting intramolecular hydrogen bond (yellow). (D) Space filling model of promysalin (green) in Sdh highlighting key lipophilic residues (magenta) and resistance mutation (orange). (E) Summary of structural changes in new promysalin analogues.

Scheme 1. General Synthetic Route for the Synthesis of New Promysalin Analogues[a]

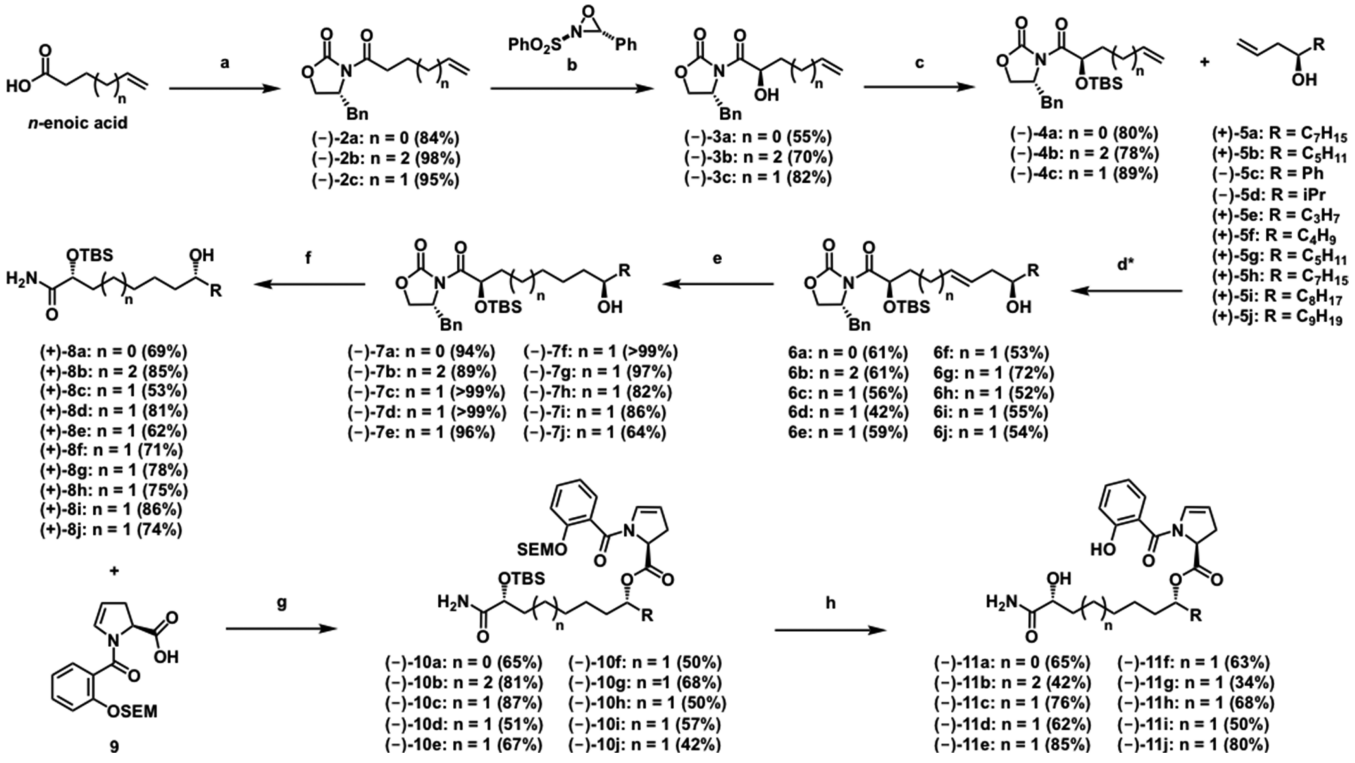

[a]Reaction conditions: (a) (i) NEt_3, PivCl, THF; (ii) LiCl, (R)- 4-benzyl-2-oxazolidinone; (b) NaHMDS, CSA; (c) TBSCl, imidazole, DMF; (d) Grubbs catalyst C711, CH_2Cl_2; *4c used to make **6c−6j**; (e) H_2, Pd/C, EtOAc; (f) NH_4OH, THF/H_2O; (g) EDC, DMAP, CH_2Cl_2; (h) TBAF, DMPU, THF.

negative and Gram-positive species.[14] Intrigued by this highly selective nature, our lab soon published the first total synthesis of the natural product.[15] We subsequently reported the diverted total synthesis of a number of structural analogues and their biological activity as summarized in Figure 1B.[16,17] Based on these findings and competing studies that postulated that promysalin targeted the cell membrane of *S. aureus*,[18] we sought to definitively identify the biological target. Our SAR investigation enabled the synthesis of a probe compound utilizing the Yao minimalist probe,[19] facilitating our subsequent target identification studies. Using affinity-based protein profiling, we identified succinate dehydrogenase (Sdh) as the biological target of promysalin in *PA*.[20] This mechanism was validated by a resistance selection assay followed by whole genome sequencing of two resulting mutants, revealing the same single nucleotide point mutation of I206V in Sdh. We had previously described the ability of promysalin to chelate iron,[16] but further transcriptomic studies

https://dx.doi.org/10.1021/acsinfecdis.0c00024
ACS Infect. Dis. XXXX, XXX, XXX−XXX

Table 1. Summary of Overall Yield and Growth Inhibition for Promysalin and Analogues against PA14[a]

	Structure	PA14 IC_{50} (μM)	PA14 IC_{90} (μM)	Overall Yield
Connectivity	(-)-11a n = 0	3.1	12	27%
	(-)-11b n = 2	5.7	22	22%
Bulky	(-)-11c n = 1	38	140	42%
	(-)-11d n = 1	130	200	20%
Truncated	(-)-11e n = 1	9.4	22	36%
	(-)-11f n = 1	5.7	21	20%
	(-)-11g n = 1	2.5	12	15%
	Gentamicin	3.6	17	--
	(-)-1	0.065	4.6	39%
Elongated	(-)-11h n = 1	0.026	0.89	22%
	(-)-11i n = 1	0.035	1.0	18%
	(-)-11j n = 1	0.15	1.6	21%

[a]Gentamicin was used as a positive control. IC_{50} and IC_{90} values are the average of three trials.

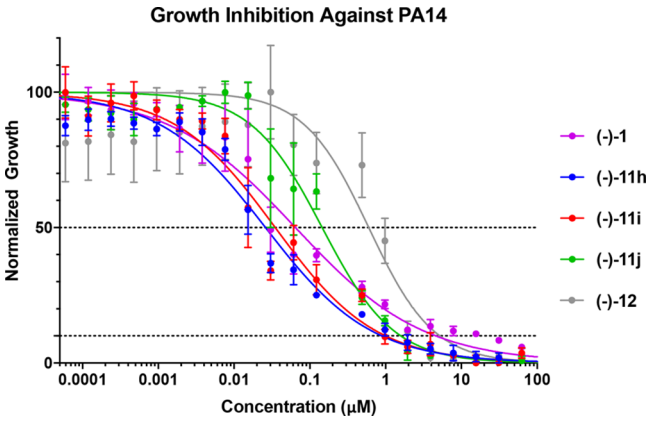

Figure 2. Inhibitory activity of promysalin and extended chain analogues against PA14. Best fit lines and data points are the average of three trials (error bars indicate SEM). Dotted lines indicate IC_{50} and IC_{90}.

by our group rationalized the antivirulence activity to also correlate to the inhibition of Sdh.[21] Interestingly, the activity and structure of promysalin is reminiscent to that of siccanin, a fungal Sdh inhibitor that was rediscovered as an antibiotic that specifically inhibits *PA*.[22,23]

With the protein target identified, we then sought to use this information to strategically design new analogues based on the structure of Sdh. Both of our target identification experiments indicated that promysalin was interacting in the ubiquinone

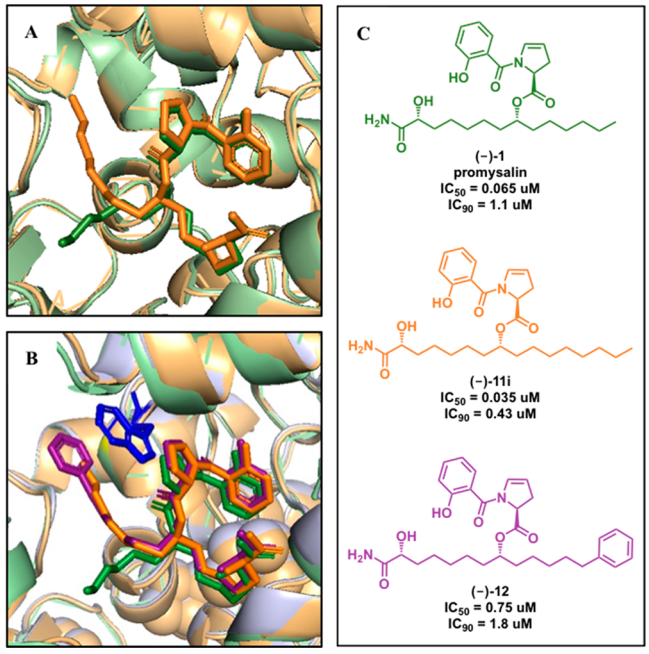

Figure 3. (A) Computational model of promysalin (green) and extended chain analogue **11i** (orange). (B) Model of promysalin, analogue **11i**, and extended aromatic analogue **12** (purple). TRP161 residue on Sdh shown in blue. (C) Structures of promysalin and analogues **11i** and **12** and their inhibitory activity against PA14.

binding site, which is in line with the mechanism of known Sdh inhibitors.[24,25] Based on this information, we carried out computational docking of promysalin using a previously characterized homologous *E. coli* model of Sdh[26] along with known binding models of other previously characterized inhibitors[27] (Figure 1C,D). This model indicated that promysalin binds with a macrocyclic conformation dictated by an intramolecular hydrogen bond between the ester and the amide, which has been reaffirmed by previous structure activity relationships (Figure 1C).[20] The model also revealed that I206 (Figure 1D, orange) has increased hydrophobic contacts with promysalin (green) as compared to ubiquinone, the native substrate. Mutation of this isoleucine to valine eliminates these key interactions (black) and results in an ~50-fold reduction in activity, revealing the importance of these contacts. With this information in hand, we wanted to design synthetic analogues that would potentially restore these interactions. Accordingly, we hypothesized that changing the position of the ester on the carbon side chain would impact this macrocyclic conformation of the molecule thereby potentially regaining contacts in the resistant strain. Additional inspection of the model showed that the aliphatic tail of promysalin is positioned in a pocket containing several hydrophobic residues (Figure 1D, magenta) that could contribute to positive binding interactions. We postulated that although nature has provided a fantastic lead compound in promysalin, it is limited in the molecular building blocks at its disposal, wherein the side chain of promysalin is derived from myristic acid. However, as organic chemists, we are limited solely by the synthetic buildings blocks available. The flexibility of our synthetic strategy provided us with the ability to manipulate the alkyl chain in order to optimize the biological activity, pharmacological profile, and potentially identify new binding modes.

https://dx.doi.org/10.1021/acsinfecdis.0c00024
ACS Infect. Dis. XXXX, XXX, XXX−XXX

To assess these hypotheses, we now synthesized a series of rationally designed structural analogues with side chains of varying length (Table 1, **11e**−**11j**) and steric bulk (**11c** and **11d**). Two additional analogues would retain the overall 14-carbon side chain but move the position of the ester from C_8 (**1**) to C_7 (**11a**) or C_9 (**11b**), which would serve to manipulate the macrocyclic conformation. Employing our previously reported synthetic route,[15] we began by installing an Evans chiral auxiliary to commercially available *n*-eneoic acids (Scheme 1). This enabled a stereoselective Davis oxidation followed by TBS protection affording various fragments with general structure **4**, where n = 0, 1, or 2. Cross metathesis with homoallylic alcohols (**5**), synthesized to accommodate a wide range of alkyl substituents, followed by hydrogenation and subsequent auxiliary removal afforded fragments with general structure **8**, where R corresponds to the alkyl tail of the final analogues (Table 1). EDC-mediated esterification with compound **9** (synthesis reported previously[15]) followed by global deprotection afforded analogues **11a**−**11j**, which were obtained in overall yields ranging from 15 to 42%.

With 10 new analogues in hand, we evaluated their inhibitory activity against the *PA* strains, PA14 and PAO1, and the resistant *PA* strain selected for in our laboratory, RO5 (Table 1, Table S1). As we expected, the activity of the linear alkyl chain analogues varied significantly with chain length. Generally, those with truncated chains relative to promysalin were less active (Table 1, **11e**−**11g**), while extending the chain by one or two carbons increased activity (**11h**, **11i**). These results indicate that the hydrophobic interactions with the alkyl tail are important for binding affinity. However, if too many carbons were added (**11j**), activity diminished, suggesting that we had achieved optimal chain length in analogue **11h**. Alternatively, adding sterically hindered or rigid groups such as phenyl (**11c**) or isopropyl (**11d**) to a truncated chain greatly reduced activity, suggesting that the binding pocket does not easily accommodate nonlinear tails. Finally, changing the position of the ester and presumably disrupting the intramolecular hydrogen bonding network, decreased activity (**11a**, **11b**), indicating that this structural feature is critical for an optimized conformation within the binding pocket. Interestingly, the activity of most analogues decreased only marginally in the resistant strain (5−12-fold decrease) relative to promysalin (∼50-fold decrease) (Table S1). However, other analogues had a greater reduction in activity compared to promysalin. Overall, a general trend was not observed between chain length and differential inhibitory activity between resistant and susceptible strains.

Upon closer inspection of the growth curves, we noticed a change in the slope for analogues with longer side chains (Figure 2). For that reason, we calculated IC_{90} values for inhibition against PA14 (Table 1), which are more clinically relevant values due to the possibility that 50% inhibition may not be sufficient for desired outcomes.[28−30] Additionally, a steeper inhibition curve indicates that small increases in concentration result in large increases in activity, making inhibition more attainable at physiologically relevant concentrations.

In order to rationalize the observed biological activity, we built computational models of these analogues in complexes with Sdh. We were surprised to find that the positioning of the alkyl chain in these models was not always the same as in promysalin. All analogues with shorter alkyl chains resulted in conformations very similar to that observed with promysalin (Figure 3A, green). However, all analogues with increased tail length were positioned such that their tail was oriented into a previously unidentified binding cleft (Figure 3A, orange), as the native orientation would unfavorably extend the hydrophobic side chain into a solvent-exposed region. We postulated that this is the driving force for the longer analogues to occupy this new region of the binding pocket.

We also identified a tryptophan residue (Trp161, Figure 3B, blue) in proximity to the alkyl chain terminus in the new binding orientation. We speculated that installing a terminal aromatic group on the side chain would induce π-stacking interactions with the protein resulting in a higher binding affinity.[31] Additional computational analysis revealed that an ideal chain length would contain six carbons between the aromatic moiety and the ester linker arriving at analogue **12** (Figure 3B, purple; Figure 3C). Analogue **12** is easily accessible via our previously described synthetic sequence in 21% overall yield, requiring only minor modifications (Scheme S1). We then examined its inhibitory activity against PA14. These results revealed that **12** has an IC_{50} = 0.75 μM and an IC_{90} = 1.8 μM. Although this is less potent than the parent compound, it is >200 fold more active than the truncated aryl analogue **11c**. This indicates that this new binding cleft is more amenable to changes, and this analogue provides a promising starting point for further optimization.

In conclusion, we have synthesized 11 promysalin analogues based on its computationally predicted binding mode in Sdh. Biological investigation of these analogues revealed that manipulating the hydrophobic character on the alkyl chain has a direct effect on growth inhibition, resulting in two analogues more potent than the natural product. Notably, a new putative binding cleft was revealed through computational modeling of Sdh, which has the ability to accommodate greater structural diversity, including both linear and rigid aromatic moieties, and leads to improved IC_{90} values. This provides the basis for future work focused on optimization of binding interactions in the newly discovered cleft combined with other improvements previously reported by our group toward the development of a potent *PA*-specific antimicrobial agent.

■ ASSOCIATED CONTENT

Supporting Information

The Supporting Information is available free of charge at https://pubs.acs.org/doi/10.1021/acsinfecdis.0c00024.

Synthetic procedures and biological assays (PDF)

■ AUTHOR INFORMATION

Corresponding Author

William M. Wuest − *Department of Chemistry and Emory Antibiotic Resistance Center, Emory School of Medicine, Emory University, Atlanta, Georgia 30322, United States;* orcid.org/0000-0002-5198-7744; Email: wwuest@emory.edu

Authors

Savannah J. Post − *Department of Chemistry, Emory University, Atlanta, Georgia 30322, United States*

Colleen E. Keohane − *Department of Chemistry, Emory University, Atlanta, Georgia 30322, United States*

Lauren M. Rossiter − *Department of Chemistry, Temple University, Philadelphia, Pennsylvania 19122, United States*

https://dx.doi.org/10.1021/acsinfecdis.0c00024
ACS Infect. Dis. XXXX, XXX, XXX−XXX

Anna R. Kaplan − *Department of Chemistry, Emory University, Atlanta, Georgia 30322, United States*
Jittasak Khowsathit − *Molecular Therapeutics Program, Fox Chase Cancer Center, Philadelphia, Pennsylvania 19111, United States*
Katie Matuska − *Department of Chemistry, Emory University, Atlanta, Georgia 30322, United States*
John Karanicolas − *Molecular Therapeutics Program, Fox Chase Cancer Center, Philadelphia, Pennsylvania 19111, United States;* orcid.org/0000-0003-0300-726X

Complete contact information is available at: https://pubs.acs.org/10.1021/acsinfecdis.0c00024

Author Contributions

[⊥]S.J.P. and C.E.K. contributed equally. The manuscript was written through contributions of all authors. All authors have given approval to the final version of the manuscript.

Notes

The authors declare the following competing financial interest(s): Intellectual property has been filed on the structures presented.

■ ACKNOWLEDGMENTS

We are grateful to the NIH (Grants GM119426 and GM123336) and NSF (Grant CHE1755698) for financial support. Partial instrumentation support was provided by the NSF (Grant CHE1531620). S.J.P and A.R.K. acknowledge National Science Foundation Pre-Doctoral Fellowships (Grant DGE1937971). We thank Umicore for olefin metathesis catalysts and Profs. Buttaro (Temple University) and Goldberg (Emory University) for the generous donation of the strains. This work used the Extreme Science and Engineering Discovery Environment (XSEDE) Allocation MCB130049, which is supported by National Science Foundation Grant Number ACI-1548562. This research was also funded in part through the NIH/NCI Cancer Center Support Grant P30 CA006927.

■ REFERENCES

(1) Ventola, C. L. (2015) The Antibiotic Resistance Crisis: Part 1: Causes and Threats. *P T 40*, 277−283.
(2) Biggest Threats and Data. *CDC's Antibiotic Resistance Threats Report*, 2019.
(3) Lewis, K. (2013) Platforms for Antibiotic Discovery. *Nat. Rev. Drug Discovery 12*, 371−387.
(4) Garland, M., Loscher, S., and Bogyo, M. (2017) Chemical Strategies To Target Bacterial Virulence. *Chem. Rev. 117*, 4422−4461.
(5) Cantón, R., and Morosini, M. I. (2011) Emergence and Spread of Antibiotic Resistance Following Exposure to Antibiotics. *FEMS Microbiol. Rev. 35*, 977−991.
(6) Heijerman, H. (2005) Infection and Inflammation in Cystic Fibrosis: A Short Review. *J. Cystic Fibrosis 4* (2), 3−5.
(7) Bhagirath, A. Y., Li, Y., Somayajula, D., Dadashi, M., Badr, S., and Duan, K. (2016) Cystic Fibrosis Lung Environment and Pseudomonas Aeruginosa Infection. *BMC Pulm. Med. 16*, 17.
(8) *Multidrug-Resistant Pseudomonas Aeruginosa*, CDC's Antibiotic Resistance Threats Report, 2019.
(9) Hopkins, S. J. (1997) *Drugs and Pharmacology for Nurses*, 12th ed., Churchill Livingstone.
(10) Crull, M. R., Ramos, K. J., Caldwell, E., Mayer-Hamblett, N., Aitken, M. L., and Goss, C. H. (2016) Change in Pseudomonas Aeruginosa Prevalence in Cystic Fibrosis Adults over Time. *BMC Pulm. Med. 16*, 176.
(11) Keohane, C. E., Steele, A. D., and Wuest, W. M. (2015) The Rhizosphere Microbiome: A Playground for Natural Product Chemists. *Synlett 26* (20), 2739−2744.
(12) Rossiter, S. E., Fletcher, M. H., and Wuest, W. M. (2017) Natural Products as Platforms to Overcome Antibiotic Resistance. *Chem. Rev. 117* (19), 12415−12474.
(13) Abouelhassan, Y., Garrison, A. T., Yang, H., Chávez-Riveros, A., Burch, G. M., and Huigens, R. W. (2019) Recent Progress in Natural-Product-Inspired Programs Aimed to Address Antibiotic Resistance and Tolerance. *J. Med. Chem. 62* (17), 7618−7642.
(14) Li, W., Estrada-De Los Santos, P., Matthijs, S., Xie, G. L., Busson, R., Cornelis, P., Rozenski, J., and De Mot, R. (2011) Promysalin, a Salicylate-Containing Pseudomonas Putida Antibiotic, Promotes Surface Colonization and Selectively Targets Other Pseudomonas. *Chem. Biol. 18* (10), 1320−1330.
(15) Steele, A. D., Knouse, K. W., Keohane, C. E., and Wuest, W. M. (2015) Total Synthesis and Biological Investigation of (−)-Promysalin. *J. Am. Chem. Soc. 137* (23), 7314−7317.
(16) Steele, A. D., Keohane, C. E., Knouse, K. W., Rossiter, S. E., Williams, S. J., and Wuest, W. M. (2016) Diverted Total Synthesis of Promysalin Analogs Demonstrates That an Iron-Binding Motif Is Responsible for Its Narrow-Spectrum Antibacterial Activity. *J. Am. Chem. Soc. 138* (18), 5833−5836.
(17) Knouse, K. W., and Wuest, W. M. (2016) The Enantioselective Synthesis and Biological Evaluation of Chimeric Promysalin Analogs Facilitated by Diverted Total Synthesis. *J. Antibiot. 69*, 337−339.
(18) Kaduskar, R. D., Scala, G. D., Al Jabri, Z. J. H., Arioli, S., Musso, L., Oggioni, M. R., Dallavalle, S., and Mora, D. (2017) Promysalin Is a Salicylate-Containing Antimicrobial with a Cell-Membrane-Disrupting Mechanism of Action on Gram-Positive Bacteria. *Sci. Rep. 7* (8861), 1−11.
(19) Li, Z., Hao, P., Li, L., Tan, C. Y. J., Cheng, X., Chen, G. Y. J., Sze, S. K., Shen, H. M., and Yao, S. Q. (2013) Design and Synthesis of Minimalist Terminal Alkyne-Containing Diazirine Photo-Crosslinkers and Their Incorporation into Kinase Inhibitors for Cell- and Tissue-Based Proteome Profiling. *Angew. Chem., Int. Ed. 52* (33), 8551−8556.
(20) Keohane, C. E., Steele, A. D., Fetzer, C., Khowsathit, J., Van Tyne, D., Moynié, L., Gilmore, M. S., Karanicolas, J., Sieber, S. A., and Wuest, W. M. (2018) Promysalin Elicits Species-Selective Inhibition of Pseudomonas Aeruginosa by Targeting Succinate Dehydrogenase. *J. Am. Chem. Soc. 140* (5), 1774−1782.
(21) Giglio, K. M., Keohane, C. E., Stodghill, P. V., Steele, A. D., Fetzer, C., Sieber, S. A., Filiatrault, M. J., and Wuest, W. M. (2018) Transcriptomic Profiling Reveals That Promysalin Alters Metabolic Flux, Motility, and Iron Regulation in Pseudomonas Putida KT2440. *ACS Infect. Dis. 4*, 1179−1187.
(22) Mogi, T., Kawakami, T., Arai, H., Igarashi, Y., Matsushita, K., Mori, M., Shiomi, K., Omura, S., Harada, S., and Kita, K. (2009) Siccanin Rediscovered as a Species-Selective Succinate Dehydrogenase Inhibitor. *J. Biochem. 146* (3), 383−387.
(23) Nose, K., and Endo, A. (1971) Mode of Action of the Antibiotic Siccanin on Intact Cells and Mitochondria of Trichophyton Mentagrophytes. *J. Bacteriol. 105* (1), 176−184.
(24) Zhu, X. L., Xiong, L., Li, H., Song, X. Y., Liu, J. J., and Yang, G. F. (2014) Computational and Experimental Insight into the Molecular Mechanism of Carboxamide Inhibitors of Succinate-Ubquinone Oxidoreductase. *ChemMedChem 9* (7), 1512−1521.
(25) Xiong, L., Li, H., Jiang, L. N., Ge, J. M., Yang, W. C., Zhu, X. L., and Yang, G. F. (2017) Structure-Based Discovery of Potential Fungicides as Succinate Ubiquinone Oxidoreductase Inhibitors. *J. Agric. Food Chem. 65*, 1021−1029.
(26) Yankovskaya, V., Horsefield, R., Törnroth, S., Luna-Chavez, C., Miyoshi, H., Léger, C., Byrne, B., Cecchini, G., and Iwata, S. (2003) Architecture of Succinate Dehydrogenase and Reactive Oxygen Species Generation. *Science (Washington, DC, U. S.) 299* (5607), 700−704.
(27) Sierotzki, H., and Scalliet, G. (2013) A Review of Current Knowledge of Resistance Aspects for the Next-Generation Succinate

Dehydrogenase Inhibitor Fungicides. *Phytopathology 103* (9), 880−887.
(28) Sampah, M. E. S., Shen, L., Jilek, B. L., and Siliciano, R. F. (2011) Dose-Response Curve Slope Is a Missing Dimension in the Analysis of HIV-1 Drug Resistance. *Proc. Natl. Acad. Sci. U. S. A. 108* (18), 7613−7618.
(29) Mammano, F., Trouplin, V., Zennou, V., and Clavel, F. (2000) Retracing the Evolutionary Pathways of Human Immunodeficiency Virus Type 1 Resistance to Protease Inhibitors: Virus Fitness in the Absence and in the Presence of Drug. *J. Virol. 74* (18), 8524−8531.
(30) Bangsberg, D. R., Kroetz, D. L., and Deeks, S. G. (2007) Adherence-Resistance Relationships to Combination HIV Antiretroviral Therapy. *Curr. HIV/AIDS Rep. 4* (2), 65−72.
(31) da Silva, C. H. T. P., Campo, V. L., Carvalho, I., and Taft, C. A. (2006) Molecular Modeling, Docking and ADMET Studies Applied to the Design of a Novel Hybrid for Treatment of Alzheimer's Disease. *J. Mol. Graphics Modell. 25* (2), 169−175.

https://dx.doi.org/10.1021/acsinfecdis.0c00024
ACS Infect. Dis. XXXX, XXX, XXX−XXX